

Imine–Enamine Tautomeric Equilibrium of Palladium Imidoyl Complexes

Juan Cámpora,* Sarah A. Hudson, Philippe Massiot, Celia M. Maya, Pilar Palma, and Ernesto Carmona*

Departamento de Química Inorgánica–Instituto de Investigaciones Químicas, Universidad de Sevilla–Consejo Superior de Investigaciones Científicas, C/ Américo Vespucio s/n, Isla de la Cartuja, 41092 Sevilla, Spain

Luis A. Martínez-Cruz and Angel Vegas*

Instituto de Química-Física Rocasolano, Departamento de Cristalografía, Consejo Superior de Investigaciones Científicas, C/ Serrano 119, E-28006 Madrid, Spain

Received July 16, 1999

The reaction of benzylpalladium complexes of type *trans*-[Pd(CH₂C₆H₄Y)(X)(PR₃)₂] (**2**) with isocyanides yields imidoyl complexes that exist in solution as equilibrium mixtures of the corresponding imine ([Pd(C(=NR')CH₂C₆H₄Y)(X)(PR₃)₂], **3-im**) and enamine ([Pd-(C(NHR')=CHC₆H₄Y)(X)(PR₃)₂], **3-en**) tautomers. While the equilibrium constant is markedly affected by the electronic effect exerted by the substituents at the phenyl ring (Y), the effect of the metal fragment is less pronounced and is dominated by steric factors. Both tautomeric forms can also be found in the solid state, and the X-ray structures of complexes of type **2**, **3-im**, and **3-en** have been determined.

Introduction

Tautomeric equilibrium is emerging as an important process in organometallic chemistry.¹ Very recently, equilibria between metal acyl hydrides and hydroxycarbene complexes^{1a} and between metal–vinylidene and π -alkyne species^{1b,c} have been demonstrated. Similar equilibria are often implicated in the stabilization of ligands that contain electronegative atoms.^{1d–f} The keto/enol or imine/enamine tautomerization of acyl² or imidoyl³ transition metal complexes has been observed in favorable cases, but in these instances the preference of the enol or enamine tautomer over the more common keto or imino form is due to the formation of hydrogen bonds or to the existence of appreciably acidic C–H bonds. Although the observation of keto/enol or imine/enamine tautomerism in simple acyl or imidoyl complexes is still uncommon, it may be related to the more familiar process well-known for organic ketones⁴ or imines.⁵ As in these organic compounds, the tautomeric

equilibrium may sometimes play an important role in the reactivity of acyl or imidoyl complexes.⁶

In this contribution we would like to describe the attainment of simple, tautomeric equilibria in palladium imidoyl complexes, [Pd]–C(=NR')CH₂Ar, that do not require any special stabilization of the enamine form, [Pd]–C(NHR')=CHAr. In our view, what makes this system unusual is the existence in solution of both tautomers in measurable concentrations, therefore allowing the determination of their relative stabilities. A preliminary report on this work has appeared;⁷ herein we address in full the factors that govern such equilibria and report in addition the crystal structure determinations of the imine and enamine forms of closely related derivatives.

Results and Discussion

Synthesis of Palladium Imidoyl Complexes. Palladium imidoyl complexes have been prepared (Scheme 2) by reaction of the corresponding benzylpalladium derivatives **2** with isocyanides. Although the parent benzyl complex Pd(CH₂Ph)Cl(PMe₃)₂, **2a**, had been previously reported by Milstein and co-workers,⁸ we

(1) (a) Casey, C. P.; Czerwinski, C. J.; Fusie, K. A.; Hayashi, R. K. *J. Am. Chem. Soc.* **1997**, *119*, 3971. (b) de los Ríos, I.; Jiménez Tenorio, M.; Puerta, M. C.; Valerga, P. *J. Am. Chem. Soc.* **1997**, *119*, 6529. (c) Wakatsuki, Y.; Koga, N.; Werner, H.; Morkuma, K. *J. Am. Chem. Soc.* **1997**, *119*, 360. (d) Albert, J.; González, A.; Granell, J.; Moragas, R.; Puerta, M. C.; Valerga, P. *Organometallics* **1997**, *16*, 3775. (e) Gosh, P.; Pramanik, A.; Chakravorty, A. *Organometallics* **1996**, *15*, 4147. (f) Fairlie, D. P.; Woon, T. C.; Wickramasinghe, A.; Willis, A. C. *Inorg. Chem.* **1994**, *33*, 6425.

(2) O'Connor, J. M.; Uhrhammer, R.; Rheingold, A. L.; Roddick, D. M. *J. Am. Chem. Soc.* **1991**, *113*, 4530.

(3) (a) Alias, F. M.; Belderrain, T. R.; Paneque, M.; Poveda, M. L.; Carmona, E. *Organometallics* **1997**, *16*, 301. (b) Alias, F. M.; Belderrain, T. R.; Paneque, M.; Poveda, M. L.; Carmona, E. *Organometallics* **1998**, *17*, 5620. (c) Veya, P.; Floriani, C.; Chiesi-Villa, A.; Rizzoli, L. *Organometallics* **1993**, *12*, 4899. (d) Henderson, W.; Kemmitt, R. D. W.; Prouse, L. J. S.; Russell, D. R. *J. Chem. Soc., Dalton Trans.* **1990**, 781. (e) Henderson, W.; McKenna, P.; Russell, D. R.; Prouse, L. J. S. *J. Chem. Soc., Dalton Trans.* **1989**, 345. (f) Bertani, R.; Castellani, C. B.; Crociani, B.; *J. Organomet. Chem.* **1984**, *269*, C15.

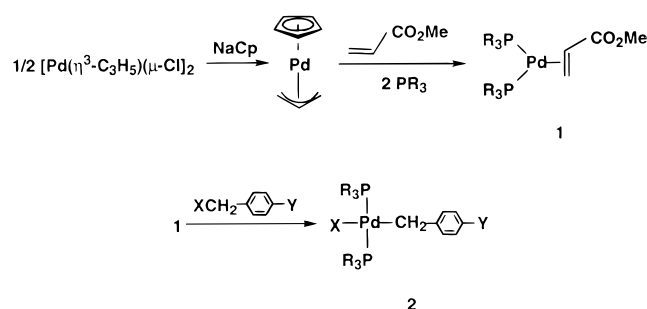
(4) (a) March, J. In *Advanced Organic Chemistry*; John Wiley: New York, 1992. (b) Häfelinger, G.; Hack, H. In *The Chemistry of Enamines*; Patai, S., Rappaport, Z., Eds.; John Wiley: New York, 1994; p 1. (c) *Enamines: Synthesis, Structure and Reactions*; Cook, A. G., Ed.; Marcel Dekker: New York, 1988.

(5) (a) de Savignac, A.; Bon, M.; Lattes, A. *Bull. Chem. Soc. Fr.* **1972**, 3167. (b) Albrecht, H.; Hanisch, H.; Funk, W.; Kalas, D. *Tetrahedron* **1972**, *28*, 5481. (c) Albrecht, H.; Fischer, S. *Tetrahedron* **1973**, *29*, 659. (d) Albrecht, H.; Funk, W.; Reiner, M. T. *Tetrahedron* **1976**, *32*, 479.

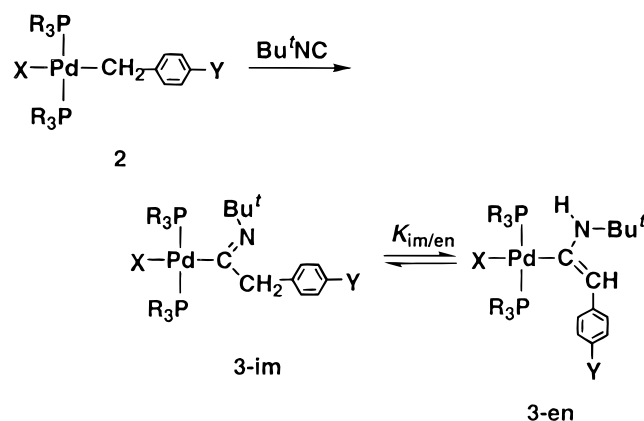
(6) Clark, H. C.; Milne, C. R. C.; Payne, N. C. *J. Am. Chem. Soc.* **1978**, *100*, 1164.

(7) Cámpora, J.; Hudson, S. A.; Carmona, E. *Organometallics* **1995**, *14*, 2151.

(8) Milstein, D. *J. Chem. Soc., Chem. Commun.* **1986**, 817.

Scheme 1

	X	PR ₃	Y
2a	Cl	PMe ₃	H
2b	Cl	PMe ₃	CF ₃
2c	Br	PMe ₃	Br
2d	Br	PMe ₃	H, <i>o</i> -Br
2e	Br	PMe ₃	NO ₂
2f	Br	PMe ₃	CN
2g	Cl	PEt ₃	CF ₃
2h	Br	PEt ₃	Br
2i	Cl	PMe ₂ Ph	CF ₃
2j	Cl	PMe ₂ (C ₆ H ₄ - <i>p</i> -NMe ₂)	CF ₃
2k	Cl	PMe ₂ (C ₆ H ₄ - <i>p</i> -F)	CF ₃
2l	Br	PMe ₂ Ph	NO ₂

Scheme 2

		PR ₃	Y
3a	Cl	PMe ₃	H
3b	Cl	PMe ₃	CF ₃
3c	Br	PMe ₃	Br
3d	Br	PMe ₃	H, <i>o</i> -Br
3e	Br	PMe ₃	NO ₂
3f	Br	PMe ₃	CN
3g	Cl	PEt ₃	CF ₃
3h	Br	PEt ₃	Br
3i	Cl	PMe ₂ Ph	CF ₃
3j	Cl	PMe ₂ (C ₆ H ₄ - <i>p</i> -NMe ₂)	CF ₃
3k	Cl	PMe ₂ (C ₆ H ₄ - <i>p</i> -F)	CF ₃
3l	Br	PMe ₂ Ph	NO ₂
3m ¹	Cl	PMe ₃	CF ₃

¹: PrⁱNC derivative

to Pd(0)–methyl acrylate complexes.⁹ The latter can be generated in situ from [Pd(η³-C₃H₅)(μ-Cl)]₂, NaCp, and PR₃ plus CH₂=CHCO₂Me (Scheme 1).¹⁰ This synthetic methodology has proved fairly general and provides access to complexes that contain different substituents on the aromatic ring and different phosphine coligands. Good results have been obtained for PMe₃, PEt₃, and arylphosphines of type PMe₂C₆H₄-*p*-X, although the PMe₂C₆H₄-*p*-F derivative, **2k**, is somewhat unstable in solution and its isolation in the solid state has proved unreliable. In general, better yields are achieved when benzyl chlorides are used instead of bromides, but both types of reagents appear to be suitable and, in practice, the use of a particular halide was often imposed only for reasons of commercial availability. Tables 1 and 2 show analytical and NMR properties for these compounds.

The reaction of compounds **2a–l** with *tert*-butyl isocyanide proceeds readily at room temperature (Scheme 2), yielding the corresponding imido complexes **3a–l** as yellow to orange solids, with the exception of the nitro derivatives **3e** and **3l**, which exhibit a remarkable green-red dichroism in the solid state, and complex **3k**, which was isolated as a yellow oil and purified by chromatography. The analogous interaction of **2b** with PrⁱNC gives the expected compound **3m** in the form of orange crystals.

In solution, these imido complexes exist as a mixture of the imino (**3-im**) and enamino (**3-en**) tautomers, which can be identified on the basis of their spectroscopic properties. The solid-state structures of the closely related imine and enamine tautomers **3c-im** and **3h-en**, which differ only in the nature of the PR₃ ligands (PMe₃ and PEt₃, respectively), have been determined by X-ray studies (see below). The chloride ligand of complexes **3a** and **3b** has been exchanged by Br[−], by metathesis with an excess of KBr, giving rise to complexes **3n** and **3o**, but as shown in Table 3, this metathesis has very little effect on the corresponding tautomeric ratios.

The ¹H and ¹³C{¹H} NMR spectra of these mixtures show the expected features for the imido and enamino functionalities (Tables 4 and 5). The iminoacyl (C=N) resonance of compounds of type **3-im** appears at δ 173–177 ppm (at somewhat lower field, 184 ppm, in the PrⁱNC complex **3m-im**). The Pd-bonded carbon atom of the enamines **3-en** resonates at higher field, in the 160–172 ppm region, whereas the β-carbon gives rise to a singlet signal between 100 and 102 ppm, i.e., the zone characteristic of organic enamines.¹¹ Although the quaternary carbon resonances of the imine or enamine functionalities (M–C) are not appreciably split by coupling with the phosphorus nuclei, they appear somewhat broad, making difficult their observation for the tautomers that are present in a low ratio.

Some of the ¹H NMR signals due to the two tautomers of each complex allow their ready quantification in the NMR spectra of the mixtures (Table 4). For instance,

(9) Cámpora, J.; Graiff, C.; Palma, P.; Carmona, E.; Tiripicchio, A. *Inorg. Chim. Acta* **1998**, *269*, 191.

(10) (a) Binger, P.; Büch, H. M.; Benn, R. Myntt, R. *Angew. Chem., Int. Ed. Engl.* **1982**, *21*, 62. (b) Schwager, H.; Bann, R.; Wilke, G. *Angew. Chem., Int. Ed. Engl.* **1987**, *26*, 67.

(11) Chiara, J. L.; Gómez-Sánchez, A. In *The Chemistry of Enamines*; Patai, S., Rappaport, Z., Eds.; John Wiley: New York, 1994; p 279.

have found that a convenient preparative route to these derivatives is the oxidative addition of benzyl halides

Table 1. Analytical and $^{31}\text{P}\{^1\text{H}\}$ and ^1H NMR Data for Benzyl Complexes

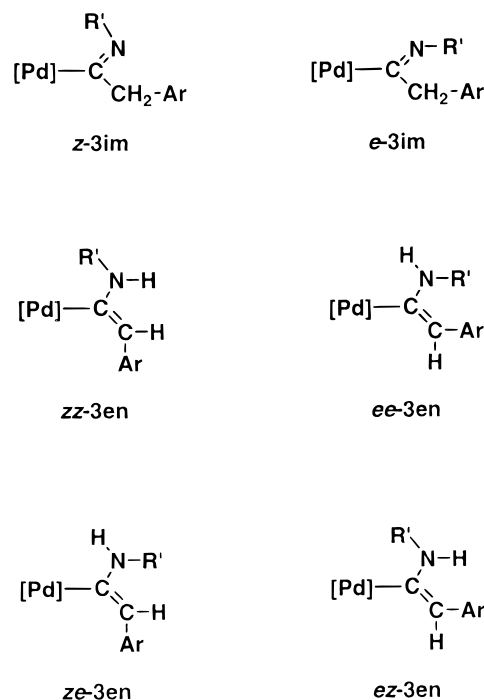
	anal. data ^a		$^{31}\text{P}\{^1\text{H}\}$	^1H NMR, δ (J, Hz) ^b		
	C	H		PR_3^c	CH_2	CH_{ar}^d
X = Cl, Y = H, R = Me, 2a ^e	40.5(40.5)	6.5(6.5)	−16.1	1.29 (t, 3.4, Me)	2.66 (t, 8.2)	6.98 (t, 1 H, 7.3) 7.06 (t, 2 H, 7.6) 7.28 (d, 2 H, 7.5)
X = Cl, Y = CF ₃ , R = Me, 2b ^f	37.6(37.1)	5.3(5.3)	−15.4	1.00 (t, 3.2, Me)	2.63 (t, 7.6)	7.24 (d, 2 H, 7.8) 7.33 (d, 2 H, 8.0)
X = Br, Y = Br, R = Me, 2c ^e	31.0(30.7)	4.8(4.7)	−17.7	1.12 (br s, Me)	2.46 (t, 8.0)	6.95 (br s, 4 H)
X = Br, Y = <i>o</i> -Br, R = Me, 2d ^g	30.5(30.7)	4.7(4.7)	−16.6	1.26 (t, 3.3, Me)	2.68 (t, 7.5)	6.87 (t, 1 H, 6.3) 7.02 (t, 1 H, 7.4) 7.34 (d, 1 H, 7.9) 7.77 (d, 1 H, 7.5)
X = Br, Y = NO ₂ , R = Me, 2e ^{h,e}	33.2(32.9)	5.2(5.1)	−20.3	1.36 (t, 3.4, Me)	2.80 (t, 7.8)	7.35 (d, 2 H, 8.1) 7.92 (d, 2 H, 8.1)
X = Br, Y = CN, R = Me, 2f ^{i,g}	37.5(37.0)	5.3(5.3)	−15.9	1.39 (t, 3.4, Me)	2.84 (t, 7.9)	7.39 (d, 2 H, 8.2) 7.43 (d, 2 H, 8.3)
X = Cl, Y = CF ₃ , R = Et, 2g ^j	44.8(44.7)	7.0(6.7)	14.3	1.08 (pq, 7.8, Me) 1.79 (ct, 7.6 ^d 3.6, CH ₂)	2.71 (t, 7.1)	7.42 (d, 2 H, 8.1) 7.60 (d, 2 H, 8.1)
X = Br, Y = Br, R = Et, 2h ^j	38.3(38.5)	5.9(6.1)	12.4	1.06 (pq, 7.8, Me) 1.84 (ct, 7.5 ^d 3.6, CH ₂)	2.71 (t, 7.2)	7.26 (d, 2 H, 8.5) 7.38 (d, 2 H, 8.4)
X = Cl, Y = CF ₃ , PR ₃ = PMe ₂ Ph, 2i ^g	49.8(49.9)	4.7(4.9)	−4.6	1.71 (t, 3.3, Me) 7.41 (m, 6 H, Ph) 7.55 (m, 4 H, Ph)	2.47 (t, 7.5)	6.80 (d, 2 H, 8.1) 7.10 (d, 2 H, 8.1)
X = Cl, Y = CF ₃ , PR ₃ = PMe ₂ Ar, 2j ^{k,g} (Ar = C ₆ H ₄ - <i>p</i> -NMe ₂)	50.3(50.7)	5.5(5.8)	5.7	1.62 (t, 2.9, Me) 2.99 (Me-N) 6.71 (t, 2 H, 8.3 ^d CH _{ar}) 7.39 (m, 2 H, CH _{ar})	2.51 (t, 7.5)	6.84 (d, 2 H, 8.0) 7.12 (d, 2 H, 7.9)
X = Br, Y = NO ₂ , PR ₃ = PMe ₂ Ph, 2l ^{l,g}	46.0(46.1)	4.7(4.7)	−5.6	1.78 (t, 3.3, Me) 7.42 (m, 6 H, Ph) 7.56 (m, 4 H, Ph)	2.56 (t, 7.2)	6.65 (d, 2 H, 8.6) 7.65 (d, 2 H, 8.7)

^a Calculated values in parentheses. ^b Singlets unless otherwise indicated. ^c Apparent or real J_{HP} . ^d J_{HH} . ^e CDCl₃. ^f C₆D₆. ^g CD₂Cl₂. ^h N: 3.0(2.9). ⁱ N: 3.1(3.1). ^j CD₃COCD₃. ^k N: 4.3(4.2). ^l N: 2.2(2.3).

in acetone-*d*₆, the imino form is characterized by a singlet resonance at δ 3.5–4.2 ppm due to the methylene group, while the vinylamino group of the enamine species gives rise to two signals at δ 4.0–6.0 ppm (broad singlet) and δ 5.4–5.9 ppm (triplet, $^4J_{\text{HP}}$ ca. 3 Hz), corresponding to the amino (NH) and vinyl (=CH–Ar) protons, respectively. The integration of directly comparable aromatic signals or, in some cases, of the resonances due to the methyl groups of the phosphine ligands of both tautomers provides an accurate measurement of the equilibrium constant (Table 3).

The ^1H and $^{13}\text{C}\{^1\text{H}\}$ spectra of both the imine and the enamine forms of compounds **3i**–**l**, which bear arylphosphines of type PMe₂(C₆H₄-*p*-X), display two resonances for the phosphine methyl groups. The diastereotopic character of these groups reveal that the bulky imidoyl or α -enamino ligands are not contained in the coordination plane and that rotation around the Pd–C bond does not take place readily at room temperature.

In principle both the enamine and the imine species are expected to occur as mixtures of geometrical isomers (Chart 1). However, only one species is observed for each tautomer. In the enamines, the splitting of the vinylic proton due to coupling to the two ^{31}P nuclei ($^4J_{\text{HP}} \approx 3$ Hz) suggests a *z* distribution of the aryl and [Pd] moieties across the C=C bond. This configuration, which allows for the conjugation of the N lone pair, the double bond, and the aromatic ring, is also the more favorable for organic secondary enamines, although for these, minor amounts of the *e*-enamine tautomer are frequently present.^{5a} Scheme 3 shows the results of

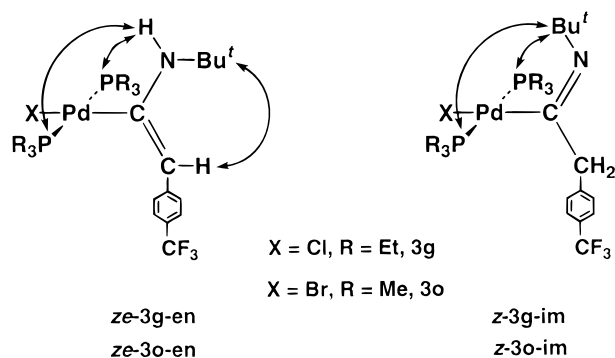
Chart 1

NOESY experiments for the tautomeric mixtures **3g-im/3g-en** and **3o-im/3o-en**. They reveal NOE cross-peaks between the vinylic and the *t*-Bu protons, in accord with a *ze* configuration, supported in addition by other NOE relationships, e.g., that between the NH

Table 2. $^{13}\text{C}\{^1\text{H}\}$ NMR Data for Benzyl Complexes^a

	PR_3^b	CH_2	aromatics
$\text{X} = \text{Cl}, \text{Y} = \text{H}, \text{R} = \text{Me}, \mathbf{2a}^c$	14.4 (t, 13.2, Me)	19.2 (t, 16.3)	121.0, 127.4, 128.9 (1, 2, 2 CH) 152.8 (C_{ar})
$\text{X} = \text{Cl}, \text{Y} = \text{CF}_3, \text{R} = \text{Me}, \mathbf{2b}^d$	18.0 (t, 14.2, Me)	21.2 (br s)	129.7 (d, 4, ^e 2 CH) 134.9 (2 CH) 130.2 (q, 32, ^e C-CF ₃) 158.4 (C_{ar})
$\text{X} = \text{Br}, \text{Y} = \text{Br}, \text{R} = \text{Me}, \mathbf{2c}^c$	14.3 (t, 14.3, Me)	19.3 (br s)	117.3 ($\text{C}_{\text{ar}}-\text{Br}$) 130.4, 131.1 (2, 2 CH) 145.9 (C_{ar})
$\text{X} = \text{Br}, \text{Y} = o\text{-Br}, \text{R} = \text{Me}, \mathbf{2d}^f$	14.4 (t, 14.6, Me)	20.5 (br s)	125.5 (C_{ar}) 126.3, 127.0, 132.1, 133.5 (4 CH) 147.8 (C_{ar})
$\text{X} = \text{Br}, \text{Y} = \text{NO}_2, \text{R} = \text{Me}, \mathbf{2e}^c$	14.5 (t, 14.7, Me)	19.7 (br s)	123.1, 129.6 (2, 2 CH) 144.4, 156.6 (2 C_{ar}) 144.4, 156.6 (2 C_{ar})
$\text{X} = \text{Br}, \text{Y} = \text{CN}, \text{R} = \text{Me}, \mathbf{2f}^f$	14.7 (t, 14.7, Me)	19.9 (br s)	107.5 (C-CN) 119.8 (CN) 130.3, 131.9 (2 CH) 154.5 (C_{ar})
$\text{X} = \text{Cl}, \text{Y} = \text{CF}_3, \text{R} = \text{Et}, \mathbf{2g}^d$	8.6 (Me) 14.8 (t, 12.4, CH_2)	g	125.1 (2 CH) 127.6 (q, 31, ^e C-CF ₃) 131.1 (2 CH) 154.6 (C_{ar})
$\text{X} = \text{Br}, \text{Y} = \text{Br}, \text{R} = \text{Et}, \mathbf{2h}^c$	8.2 (Me) 14.6 (t, 12.8, CH_2)	16.8 (br s)	117.6 (C_{ar}) 130.2, 131.8 (2, 2 CH) 146.6 (C_{ar})
$\text{X} = \text{Cl}, \text{Y} = \text{CF}_3, \text{PR}_3 = \text{PMe}_2\text{Ph}, \mathbf{2i}^f$	13.1 (t, 14.4, Me) 128.8 (t, 4.6, 4 CH) 130.1 (2 CH) 131.5 (t, 5.8, 4 CH) 134.6 (t, 20.7, 2 $\text{C}_{\text{ar}}-\text{P}$)	20.5 (br s)	124.4 (q, 3.7, 2 CH) 125.1 (q, 271.3, CF ₃) 125.7 (q, 31.9, C-CF ₃) 129.3 (2 CH) 151.9 (C_{ar})
$\text{X} = \text{Cl}, \text{Y} = \text{CF}_3, \text{PR}_3 = \text{PMe}_2\text{Ar}, \mathbf{2j}^f$ (Ar = $\text{C}_6\text{H}_4-p\text{-NMe}_2$)	13.7 (t, 14.4, Me) 40.2 (Me-N) 112.1 (t, 5.1, 4 CH) 118.6 (t, 24.4, 2 $\text{C}_{\text{ar}}-\text{P}$) 132.8 (t, 6.6, 4 CH) 151.8 (2 $\text{C}_{\text{ar}}-\text{N}$)	20.9 (br s)	124.4 (q, 3.4, ^e 2 CH) 125.3 (q, 31.9, C-CF ₃) 129.3 (2 CH) 125.3 (q, 271.2, CF ₃) 152.5 (C_{ar})
$\text{X} = \text{Br}, \text{Y} = \text{NO}_2, \text{PR}_3 = \text{PMe}_2\text{Ph}, \mathbf{2l}^f$	14.5 (t, 14.8, Me) 128.8 (t, 4.4, 4 CH) 130.3 (2 CH) 131.6 (t, 5.6, 4 CH) 134.4 (t, 20.9, 2 $\text{C}_{\text{ar}}-\text{P}$)	23.8 (br s)	122.9, 129.1 (2, 2 CH) 144.3, 156.3 (2 C_{ar})

^a Singlets unless otherwise indicated. ^b Apparent or real J_{CP} . ^c CDCl_3 . ^d CD_3COCD_3 . ^e J_{CF} . ^f CD_2Cl_2 . ^g Not observed.

Scheme 3

resonance and the signals associated with the PR_3 alkyl groups. For the imines, the observation of cross-peaks between the *t*-Bu protons and those of the PR_3 ligands and the absence of such effects between the former and the methylene protons of the iminoacyl ligand are suggestive of a *z*-type conformation. Although 2D-NOESY experiments have not been recorded for every

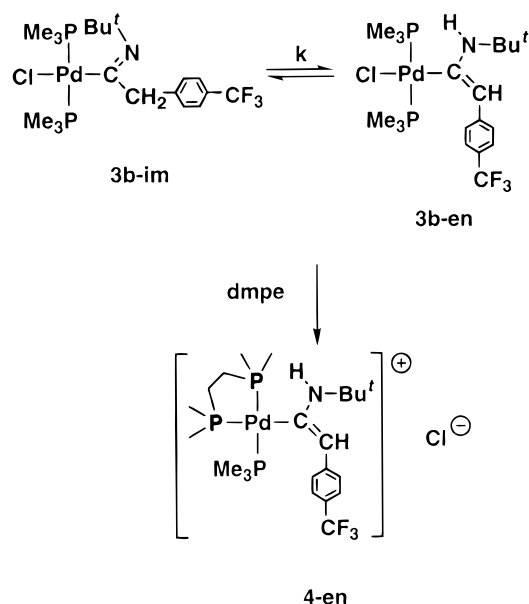
3-im/3-en tautomeric mixture, the fact that only one geometric isomer is always observed for each tautomeric form and the similarity of the NMR spectra suggest that the same geometries are adopted by each pair of tautomers.

The IR spectrum of solid samples of compounds of type **3** usually display absorption bands due to either the imine or the enamine tautomer. As found in related iminoacyl complexes of Ni,¹² imidoyl absorptions ($\nu_{\text{C}=\text{N}}$) occur at ca. 1630 cm^{-1} , and two or more bands may be observed. Although the band associated with the vinyl stretch $\nu_{\text{C}=\text{C}}$ is difficult to assign, the presence of the enamine tautomer is unequivocally revealed by the characteristic N-H absorption at ca. 3400 cm^{-1} . These IR studies show that when the imine and the enamine forms have comparable stability, sample crystallization may result in variable composition mixtures of the tautomers or even in the unexpected isolation of one pure tautomer. For example under seemingly similar

Table 3. Analytical and IR Data and Imine:Enamine Ratio^a for Imidoyl Complexes

	anal. data ^b			isolated tautomer	IR		<i>K</i> _{im/en}
	C	H	N		$\nu(\text{NH})^c$	$\nu(\text{C}=\text{N})^c$	
X = Cl, Y = H, R = Me, 3a	46.5(46.2)	7.5(7.3)	2.8(3.0)	im		1637	12.0
X = Cl, Y = CF ₃ , R = Me, 3b	42.3(42.5)	6.0(6.2)	2.6(2.6)	im + en	3340	1633, 1610	0.7
X = Br, Y = Br, R = Me, 3c	36.8(36.5)	5.9(5.6)	2.2(2.4)	im		1635	3.5
X = Br, Y = <i>o</i> -Br, R = Me, 3d	36.6(36.5)	6.0(5.6)	2.5(2.4)	im		1620	3.2
X = Br, Y = NO ₂ , R = Me, 3e	38.3(38.7)	5.8(5.9)	5.1(5.0)	en	3370		<0.1
X = Br, Y = CN, R = Me, 3f	42.4(42.4)	6.1(6.1)	5.3(5.2)	en	3407		0.1
X = Cl, Y = CF ₃ , R = Et, 3g	48.3(48.4)	7.3(7.3)	2.5(2.3)	en	3440		<0.1
X = Br, Y = Br, R = Et, 3h	42.4(42.6)	6.6(6.7)	2.1(2.1)	en	3440		0.2
X = Cl, Y = CF ₃ , PR ₃ = PMe ₂ Ph, 3i	52.8(52.7)	5.5(5.6)	2.3(2.1)	en	3430		0.3
X = Cl, Y = CF ₃ , PR ₃ = PMe ₂ Ar, 3j (Ar = C ₆ H ₄ - <i>p</i> -NMe ₂)	53.0(53.1)	6.2(6.3)	5.7(5.6)	en	3422		0.4
X = Cl, Y = CF ₃ , PR ₃ = PMe ₂ Ar, 3k (Ar = C ₆ H ₄ - <i>p</i> -F)							0.3
X = Br, Y = NO ₂ , PR ₃ = PMe ₂ Ph, 3l	49.5(49.3)	5.5(5.5)	4.2(4.1)	en	3419		0.1
X = Cl, Y = CF ₃ , R = Me, 3m ^d	41.4(41.4)	6.2(5.9)	2.6(2.7)	im		1640, 1615	6.7
X = Br, Y = H, R = Me, 3n	42.2(42.1)	6.7(6.6)	2.7(2.7)	im		1614, 1596	10.0
X = Br, Y = CF ₃ , R = Me, 3o	39.4(39.3)	5.8(5.7)	2.6(2.4)	im + en	3340	1633, 1610	0.8

^a Acetone-*d*₆. ^b Calculated values in parentheses. ^c Nujol mull, cm⁻¹. ^d PrⁿNC derivative.

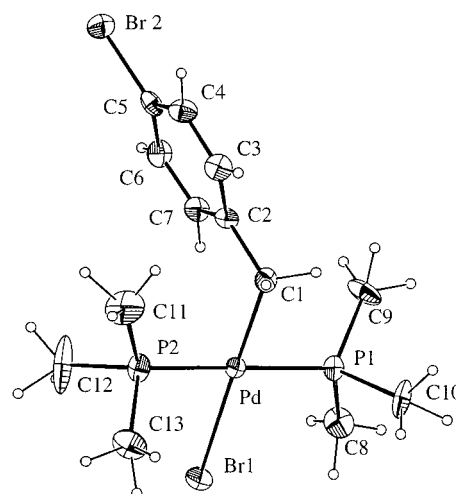
Scheme 4

conditions, different batches of compound **3b** sometimes afforded pure crystalline samples of either the imine or the enamine tautomers.

It is worth mentioning at this point that the reaction of compound **3b** with the chelating phosphine 1,2-bis-(dimethylphosphino)ethane (dmpe) affords a cationic complex **4** (Scheme 4), for which IR and NMR data demonstrate the presence of only the enamine form, both in solution and in the solid state.

Crystal Structures of Compounds 2c, 3c-im, and 3h-en. Figures 1, 2, and 3 show the crystal structures of compounds **2c**, **3c-im**, and **3h-en**, respectively. Selected bond distances and angles are summarized in Tables 8–10.

The structures of all three compounds show a Pd atom

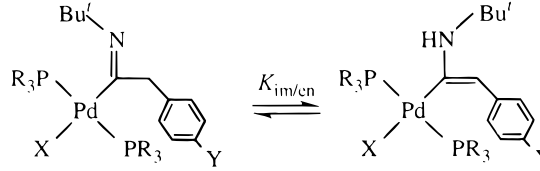
**Figure 1.** ORTEP view and atom-labeling scheme of compound **2c**.

in a slightly distorted square-planar environment, with the phosphine ligands occupying mutually trans positions. The distances and angles in compound **2c** are as expected for a *trans*-Pd(R)X(PR₃)₂ complex.¹³ Its Pd–C bond length (2.078(13) Å) is within the range expected for this functionality (2.03–2.07 Å) and very close to the Pd–C distance found in *trans*-Pd(Et)Br(PMe₃)₂¹⁴ (2.063(5) Å). However, the latter compound shows a Pd–Br bond length that is ca. 0.03 Å longer than that of **2c**, reflecting a somewhat smaller trans influence of the 4-bromobenzyl group as compared to the ethyl ligand.

As can be readily seen from Figures 2 and 3, compounds **3c** and **3h** crystallize in different tautomeric forms. Compound **3c** appears as the imine tautomer,

(13) Canty, A. J. In *Comprehensive Organometallic Chemistry*; Abel, E. W., Stone, F. G. A., Wilkinson, G., Eds.; Pergamon: New York, 1995; Vol. 9, p 225.

(14) Osakada, K.; Ozawa, Y.; Yamamoto, A. *J. Chem. Soc., Dalton Trans.* **1991**, 759.

Table 4. $^{31}\text{P}\{^1\text{H}\}$ and ^1H NMR Data for Imidoyl Complexes^a


	imine					enamine					
	$^{31}\text{P}\{^1\text{H}\}$	^1H NMR, δ (J, Hz)				$^{31}\text{P}\{^1\text{H}\}$	^1H NMR, δ (J, Hz)				
		PR_3^b	Bu^t	CH_2	CH_{ar}^c		PR_3^b	Bu^t	CH^d	NH	CH_{ar}^c
3a^e	-18.0	1.23 (t, 3.6, Me)	1.39	3.82	7.17 (tm, 1H, 7.4) 7.27 (t, 2H, 7.5) 7.46 (dm, 2H, 7.5)	-17.9	1.30 (t, 3.4, Me)	1.38	5.60 (t, 3.1)	4.69 (br s)	6.76 (tm, 1H, 7.2) 7.07 (tm, 2H, 7.8) 7.94 (d, 2H, 7.2)
3b^e	-18.2	1.31 (t, 3.3, Me)	1.36	3.94	7.59 (4H)	-17.7	1.33 (t, 3.6, Me)	1.42	5.70 (t, 2.9)	5.21 (br s)	7.33 (d, 2H, 8.4) 8.13 (d, 2H, 8.3)
3c^e	-19.9	1.37 (t, 3.8, Me)	1.36	3.82	7.33 (dm, 2H, 8.6) 7.42 (dm, 2H, 8.5)	-19.4	1.37 (t, 3.5, Me)	1.40	5.62 (t, 3.2)	4.91 (br s)	7.18 (dm, 2H, 8.7) 7.91 (dm, 2H, 8.6)
3d^e	-20.0	1.37 (t, 3.3, Me)	1.38	4.20	7.11 (tm, 1H, 7.8) 7.28 (tm, 1H, 9.0) 7.55 (dm, 1H, 9.0) 7.60 (dm, 1H, 8.5)	-20.1	1.30 (t, 3.6, Me)	1.45	5.93 (t, 3.0)	5.50 (br s)	6.68 (tm, 1H, 8.3) 7.39 (dm, 1H, 7.0) 9.10 (dm, 1H, 8.2)
3e^e	-20.0	<i>f</i>	<i>f</i>	4.04	7.29 (bd, 2H) 7.59 (bd, 2H)	-19.4	1.41 (t, 3.8, Me)	1.46	5.88 (t, 3.0)	6.04 (br s)	7.91 (dm, 2H, 8.0) 8.10 (bd, 2H, 8.4)
3f^e	-18.1	1.41 (t, 3.5, Me)	1.35	3.96	7.54 (d, 2H, 8.3) 7.64 (d, 2H, 8.3)	-19.9	1.38 (t, 7.5, Me)	1.43	5.73 (t, 3.1)	5.52 (br s)	7.33 (d, 2H, 8.8) 8.08 (d, 2H, 8.4)
3g^e	9.9	1.09 (pq, 7.0, Me)	<i>f</i>	3.59	7.42 (d, 2H, 8.2) 7.60 (d, 2H, 7.8)	10.0	1.08 (pq, 8.1, Me) 1.75 (m, 1H, CH ₂) 1.90 (m, 1H, CH ₂)	1.41	5.69 (t, 2.8)	4.44 (br s)	7.31 (d, 2H, 8.1) 8.15 (d, 2H, 8.2)
3h^e	-19.4	1.12 (pq, 7.8, Me)	1.35	3.77	7.26 (d, 2H, 8.0) 7.28 (d, 2H, 8.0)	-19.9	1.00 (pq, 7.8, Me) 1.75 (m, 1H, CH ₂) 1.85 (m, 1H, CH ₂)	1.31	5.44 (t, 3.5)	3.99 (br s)	7.11 (d, 2H, 8.0) 7.79 (d, 2H, 8.0)
3i^e	-10.5	1.62 (t, 6H, 3.3, Me) 7.49 (m, 6H, Ph) 8.05 (m, 4H, Ph)	1.28	3.85	7.77 (d, 2H, 7.9)	-9.5	1.56 (t, 6H, 3.6, Me) 1.73 (t, 6H, 3.7, Me) 7.35 (m, 6H, Ph) 7.72 (m, 4H, Ph)	1.05	5.59 (t, 3.3)	4.18 (br s)	7.22 (d, 2H, 8.3) 8.04 (d, 2H, 8.3)
3j^e	-13.1	1.54 (t, 6H, 3.3, Me) 1.63 (t, 6H, 4.1, Me) 2.99 (Me-N) 6.77 (d, 4H, 8.7, CH) 7.89 (m, 4H, CH)	1.30	3.82	7.25 (d, 2H, 8.3) 7.40 (d, 2H, 8.1)	-11.8	1.47 (t, 6H, 3.6, Me) 1.65 (t, 6H, 3.6, Me) 2.95 (Me-N) 6.72 (d, 4H, 8.7, CH) 7.59 (m, 4H, CH)	1.06	5.58 (t, 3.1)	4.09 (br s)	7.25 (d, 2H, 8.3) 8.09 (d, 2H, 8.3)
3k^e	-10.3	7.25 (d, 4H, 8.8, CH) 8.16 (m, 4H, CH)	1.30	3.90	7.33 (d, 2H, 8.1) 7.43 (d, 2H, 8.2)	-9.6	1.61 (t, 6H, 3.7, Me) 1.75 (t, 6H, 3.8, Me) 7.13 (q, 4H, 8.4, CH) 7.76 (m, 4H, CH)	1.15	5.60 (t, 3.3)	4.47 (br s)	7.19 (d, 2H, 8.5) 7.99 (d, 2H, 8.2)
3l^e	-10.8	1.57 (br t, 6H, Me) 1.76 (br t, 6H, Me)	<i>f</i>	3.86	<i>f</i>	-11.7	1.64 (t, 6H, 3.6, Me) 1.84 (t, 6H, 3.7, Me) 7.36 (m, 6H, CH) 7.71 (m, 4H, CH)	1.09	5.72 (t, 3.3)	4.93 (br s)	7.75 (d, 2H, 9.3) 7.96 (br s, 2H)
3m^{e,g}	-16.6	1.29 (t, 3.0, Me)	<i>h</i>	3.82	7.65 (s, 4H)	-17.1	1.31 (t, 3.8, Me)	<i>i</i>	5.52 (t, 2.6)	5.39 (br s)	7.26 (d, 2H, 8.0) 8.04 (d, 2H, 8.1)
3n^e		1.31 (t, 3.5, Me)	1.38	3.84	7.17 (tm, 1H, 8.7) 7.27 (tm, 2H, 8.4) 7.43 (dm, 2H, 7.3)	<i>f</i>	<i>f</i>	<i>f</i>	5.65 (t, 3.4)	4.70 (br s)	6.76 (tm, 1H, 8.0) 7.07 (tm, 2H, 7.9) 7.93 (d, 2H, 8.0)
3o^e	-20.0	1.39 (t, 3.0, Me)	1.36	3.96	7.59 (4H)	-19.5	1.38 (t, 3.0, Me)	1.42	5.73 (t, 3.2)	5.24 (br s)	7.33 (d, 2H, 8.4) 8.10 (d, 2H, 8.3)

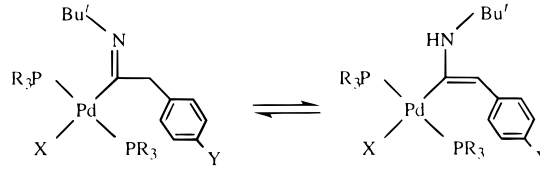
^a Singlets, unless otherwise indicated. ^b Apparent or real J_{HP} . ^c $^3J_{\text{HH}}$. ^d $^4J_{\text{HP}}$. ^e CD_3COCD_3 . ^f Not observed. ^g CNPr^i derivative. ^h Imine: 1.11 (d, $^3J_{\text{HH}} = 6.3$, Me), 3.78 (ht, $^3J_{\text{HH}} = 6.3$, $^5J_{\text{HP}} = 0.9$, CH). ⁱ Enamine: 1.22 (d, $^3J_{\text{HH}} = 6.4$, Me).

whereas the enamine form is adopted by the crystals of **3h**. In both cases, the crystalline tautomer obtained is coincident with the prevailing tautomeric form observed in solution. The plane formed by the nitrogen atom (N1) and the α - and β -carbons (C1 and C2, respectively) of the organic functionality of **3c-im** and **3h-en** is nearly perpendicular to the palladium coordination plane. It seems likely that this arrangement is adopted in order to minimize steric repulsions, but it could also be argued that such a spatial distribution could in addition allow some degree of $d\pi-\pi^*$ back-bonding interaction between the metal center and the organic fragment. This, however, is not evident at all from other crystallographic data. Thus, whereas the Pd-C bond distances of 2.012(4) and 2.05(2) Å (**3c-im** and **3h-en**, respectively) are slightly shorter than the value calculated for a Pd-C(sp²) bond (2.25 Å) and comparable to the dis-

tances found in palladium aminocarbene complexes,^{9,15} the C=N (1.24(2) Å) and C=C (1.39(2) Å) distances in **3c-im** and **3h-en** are very similar to those found in related organic imines^{4a} and enamines,^{4b} respectively, indicating that the electron back-donation from the metal to the ligand is very small, if it occurs at all.

The organic iminoacyl and enamine moieties of **3c-im** and **3h-en** are essentially planar and display *z* and *ze* conformations, respectively, as previously deduced from the spectroscopic data. The aromatic ring of **3h-en** is coplanar with the N(1)-C(1)-C(2) fragment. This may suggest that the electronic π -systems of the aromatic ring, the double bond, and the lone pair of the nitrogen atom are all conjugated,^{5b} an assumption that

(15) Dixon, K. R.; Dixon, A. C. In *Comprehensive Organometallic Chemistry*; Abel, E. W., Stone, F. G. A., Wilkinson, G., Eds.; Pergamon: New York, 1995; Vol. 9, p 193.

Table 5. $^{13}\text{C}\{^1\text{H}\}$ NMR Data for Imidoyl Complexes^a


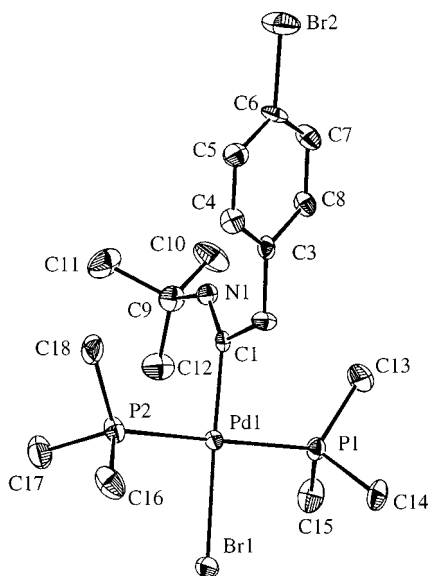
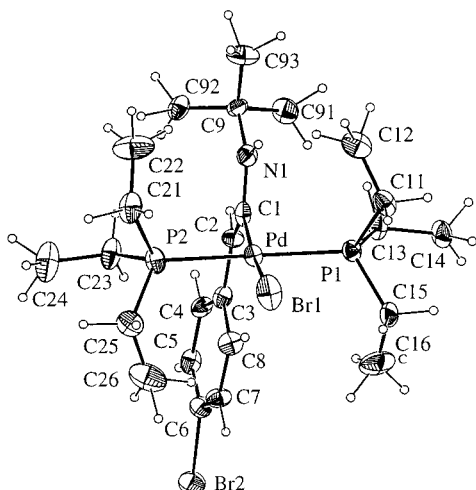
	imine					enamine				
	PR ₃ ^b	Bu ^t	CH ₂ ^c	aromatics	CN	PR ₃ ^b	Bu ^t	CH	aromatics	CN
3a^d	14.9 (t,13.5,Me)	31.0 (Me) 56.0 (C-Me)	56.0 (t,12.5)	126.2 (1CH) 128.1 (2CH) 130.5 (2CH) 138.3 (C _{ar})	176.9	13.7 (t,14.2,Me)	29.8 (Me) 52.5 (C-Me)	101.8	121.3 (1CH) 123.6 (2CH) 127.9 (2CH) 143.0 (C _{ar})	<i>e</i>
3b^f	14.7 (t,14.0,Me)	31.3 (Me) 56.4 (C-Me)	55.4 (t,13.0)	125.3 (2CH) 131.6 (2CH) 144.6 (C _{ar})	175.9	13.6 (t,14.4,Me)	30.6 (Me) 53.7 (C-Me)	101.0	121.4 (q,32, ^g C-CF ₃) 123.6 (2CH) 125.2 (2CH) 149.2 (C _{ar})	166.2
3c^f	15.6 (t,14.0,Me)	31.4 (Me) 56.8 (C-Me)	54.6 (t,13.3)	120.0 (C-Br) 131.5 (2CH) 133.2 (2CH) 139.1 (C _{ar})	<i>e</i>	14.5 (t,14.3,Me)	<i>e</i> 53.6 (C-Me)	100.7	125.9 (2CH) 131.2 (2CH) 136.0 (C _{ar})	<i>e</i>
3d^d	15.8 (t,13.8,Me)	31.0 (Me) 56.3 (C-Me)	54.6 (t,13.2)	122.5 (C _{ar}) 127.1 (1CH) 127.9 (1CH) 132.6 (1CH) 132.7 (1CH) 141.9 (C _{ar})	174.5	14.5 (t,14.7,Me)	29.5 (Me) 53.0 (C-Me)	101.2	122.3 (C _{ar}) 125.5 (1CH) 137.8 (1CH) 147.1 (C _{ar})	
3e^f						14.5 (t,15.2,Me)	30.0(Me) 54.8 (C-Me)	102.7	122.7 (2CH) 124.8 (2CH) 140.5 (C _{ar}) 152.7 (C-NO ₂)	
3f^f	15.5 (t,14.1,Me)	31.3 (Me) 57.0 (C-Me)	55.1 (t,13.5)	110.2 (C-CN) 119.7 (CN) 132.1 (2CH) 132.2 (2CH) 145.6 (C _{ar})	<i>e</i>	14.5 (t,15.1,Me)	30.0 (Me) 54.2 (C-Me)	101.8 (t,3.5)	102.0 (C-CN) 121.2 (CN) 123.8 (2CH) 132.3 (2CH) 150.0 (C _{ar})	170.7 (t, 3.6)
3g^f						8.5 (Me) 14.9 (t,12.8,CH ₂)	29.8 (Me) 53.6 (C-Me)	102.0	124.5 (2CH) 125.2 (2CH) 148.9 (C _{ar})	164.4
3h^d	8.8 (Me) 16.5 (t,11.5,CH ₂)	30.7 (Me) <i>e</i>	<i>e</i>	130.2 (2CH) 130.3 (2CH) 131.5 (C _{ar})	176.5	8.3 (Me) 14.6 (t,13.1,CH ₂)	29.7 (Me) 52.6 (C-Me)	101.0	113.3 (C-Br) 125.1 (2CH) 130.5 (2CH) 142.2 (C _{ar})	159.8
3i^h	14.2 (t,13.7,2Me) 14.9 (t,12.9,2Me) 124.6 (d,2CH) 132.4 (t,6.0,4CH)	31.1 (Me) <i>e</i>	<i>e</i>	130.4 (2CH) 130.7 (2CH)	<i>e</i>	11.3 (t,15.2,2Me) 13.3 (t,15.2,2Me) 125.1 (d,3.6,2CH) 128.7 (t,4.5,4CH) 131.1 (t,5.7,4CH) 135.2 (t,21.3,2C _{ar})	29.3 (Me) 53.2 (C-Me)	101.0	121.6 (q,32, ^g C-CF ₃) 123.2 (2CH) 130.0 (2CH) 147.6 (C _{ar})	163.0
3j^f	14.6 (t,13.9,2Me) 15.5 (t,13.5,2Me) 40.2 (4Me-N) 112.6 (m,5.3,4CH) 120.2 (t,24.2,2C-P) 134.5 (t,6.9,4CH) 144.5 (2C-N)	31.4 (Me) 56.8 (C-Me)	54.6 (t,13.9)	124.7 (pq,3.5, ^g 2CH) 127.8 (q,32.0, ^g C-CF ₃) 131.5 (2CH) 152.5 (C _{ar})	174.9 (t,6.7)	11.7 (t,15.4,2Me) 14.3 (t,15.2,2Me) 40.2 (4Me-N) 112.6 (m,5.3,4CH) 120.0 (t,25.1,2C-P) 133.3 (t,6.7,4CH) 149.2 (2C-N)	29.6 (Me) 53.5 (C-Me)	101.0 (pt,2.7)	121.5 (q,31.6, ^g C-CF ₃) 123.7 (2CH) 125.3 (pq,3.7, ^g 2CH) 130.1 (q,269.9,CF ₃) 152.4 (C _{ar})	166.7 (t,4.1)
3k^f	14.2 (t,13.8,2Me) 15.1 (t,13.3,2Me) 130.0 (4CH) 135.8 (4CH) 164.7 (d,249.2,2C-F)	31.3 (Me) 57.0 (C-Me)	54.4 (t,14.5)	124.9 (pq,3.6, ^g 2CH) 131.5 (2CH) 144.0 (C _{ar})	173.0	12.0 (t,15.2,2Me) 13.2 (t,15.2,2Me) 116.1 (m,4CH) 131.9 (t,20.7,2C-P) 134.5 (m,4CH) 164.5 (d,248.4,2C-F)	29.6 (Me) 53.7 (C-Me)	101.3 (pt,3.2)	121.9 (q,31.8, ^g C-CF ₃) 123.9 (2CH) 125.2 (pq,3.6, ^g 2CH) 126.3 (q,269.8, ^g CF ₃) 148.5 (C _{ar})	164.6
3l^h						12.0 (t,15.5,2Me) 14.9 (t,2C,15.7,Me) 128.6 (t,4.7,4CH) 130.2 (2CH) 131.2 (t,5.7,4CH) 134.8 (t,21.9,2C _{ar})	29.2 (Me) 54.1 (C-Me)	102.4 (t,3.0)	122.3 (2CH) 124.5 (2CH) 140.8 (C _{ar}) 151.4 (C-NO ₂)	172 (t,3.6)
3m^{f,i}	14.9 (t,14.3,Me)	<i>j</i>	54.4 (t,8.7)	125.6 (2CH) 131.7 (2CH) 144.7 (C _{ar})	183.9	13.6 (t,15.0,Me)	<i>k</i>	97.9	123.6 (2CH) 125.3 (2CH) 149.3 (C _{ar})	
3n^f	15.6 (t,14.0,Me)	31.4 (Me)	56.1 (pt)	126.8 (1CH) 128.7 (2CH) 131.3 (2CH) 139.7 (C _{ar})	<i>e</i>					
3o^f	15.5 (t,14.0,Me)	31.3 (Me) 56.8 (C-Me)	54.9 (t,14.1)	125.3 (2CH) 131.7 (2CH) 144.5 (C _{ar})	175.1	14.4 (t,14.3,Me)	<i>e</i> 53.8 (C-Me)	101.1	123.7 (2CH) 125.3 (2CH) 149.2 (C _{ar})	167.6

^a Singlets unless otherwise indicated. ^b Apparent or real J_{CP} . ^c $^3J_{\text{CP}}$. ^d CDCl_3 . ^e Not observed. ^f CD_3COCD_3 . ^g J_{CF} . ^h CD_2Cl_2 . ⁱ CNPr^i derivative. ^j Imine: 24.3 (Me), 60.2 (t, $^4J_{\text{CP}}$ = 6.7, CH). ^k Enamine: 23.3 (Me).

Table 6. Electronic and Steric Properties of Phosphine Ligands and $K_{\text{im/en}}$ Values

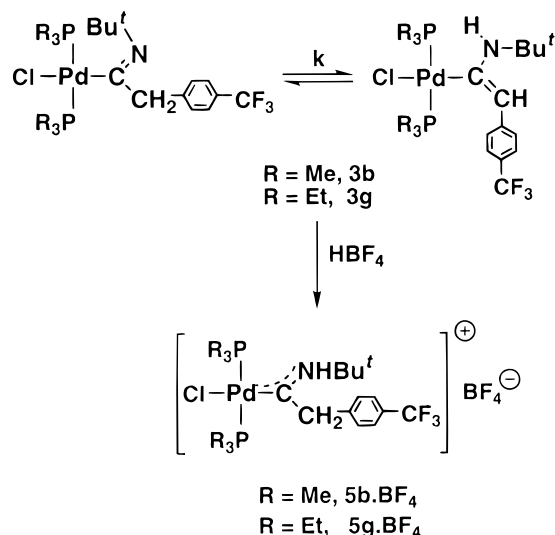
phosphine	$\nu(\text{CO})$ $\text{Ni}(\text{CO})_3(\text{PR}_3)^a$	cone angle ²⁴	$K_{\text{im/en}}^b$
PEt ₃	2061.7	132	<0.1 (3g)
PMe ₃	2064.1	118	0.7 (3b)
PMe ₂ - <i>p</i> -C ₆ H ₄ NMe ₂	2061.7	~122	0.4 (3j)
PMe ₂ Ph	2065.3	122	0.3 (3i)
PMe ₂ - <i>p</i> -C ₆ H ₄ F	2066.3	~122	0.3 (3k)

^a Calculated from data found in ref 23. ^b For complexes with X = Cl, Y = CF₃.

**Figure 2.** ORTEP view and atom-labeling scheme of compound **3c-im**.**Figure 3.** ORTEP view and atom-labeling scheme of compound **3h-en**.

is in agreement with the nearly planar configuration of the nitrogen atom.

A striking structural difference between compounds **3c-im** and **3h-en** is the contrasting geometrical disposition of the *t*-Bu substituent with respect to the palladium atom. In the latter complex, the *t*-Bu group and the bulky metal fragment are in the *e* configuration (see structure **ze-3en** of Chart 1), possibly to avoid unfavorable steric interactions. However, **3c-im** displays the opposite geometry, with the metal fragment and the nitrogen substituent adopting a *z* distribution (see structure **z-3im** of Chart 1). A survey of crystallographi-

Scheme 5

cally characterized transition metal η^1 -imidoyl complexes in the Cambridge Structural Database has shown that this arrangement is by far the most common, with 33 structures versus only four examples in which the metal fragment is placed in trans position with respect to the nitrogen substituent.¹⁶ For late transition metals (Co, Rh, Ni, Pd, and Pt), only the *z* configuration could be found. While the widespread occurrence of the *z* conformation might have in some cases a kinetic origin (i.e., stereospecific insertion of the isocyanide into the metal–carbon bond), the isomerization of the imidoyl group from the syn (*z* in the terminology used in this paper) to the anti (i.e., *e*) conformation, which is observed¹⁷ in the splitting of the imidoyl bridges of $\text{Pd}_2[\mu-(\text{C}(\text{=NMe})\text{C}_6\text{F}_5)]\text{Cl}_2(\text{CNMe})_2$ to give *trans*- $\text{Pd}(\text{C}(\text{=NMe})\text{C}_6\text{F}_5)\text{Cl}(\text{CNMe})_2$, suggests that the thermodynamic predominance of the *z* configuration (syn conformer) may be due to electronic rather than to steric factors. In contrast with this allegedly well-defined stereochemical preference, enamine derivatives and other complexes that contain α -NHR groups (e.g., cationic aminocarbenes, vide infra) do not appear to exhibit such a geometrical choice. As a way of an example, we have recently reported some enamine complexes of Pd and Pt in which the *z* and *e* conformers exist in equilibrium in solution.^{3b}

Protonation of Imidoyl/Enamine Ligands. Since η^1 -imidoyl complexes are readily protonated by acids,^{12,18} we have studied this reactivity with the aid of compounds **3b** and **3g**. Both react instantly with HBF_4 to give the cationic aminocarbene derivatives **5b**· BF_4 and **5g**· BF_4 in quantitative yield (Scheme 5).

Interestingly, complex **5g**· BF_4 seems to adopt different conformations in the solid state and in solution.

(16) (a) Andrinov, V. G.; Khomutov, M. A.; Zlotina, I. B.; Kolobova, E. N.; Struchkov, Yu. T. *Koord. Khim.* **1979**, *5*, 283. (b) Beckhaus, R.; Wagner, T.; Zimmermann, C.; Herdtweck, E. *J. Organomet. Chem.* **1993**, *460*, 181. (c) Fandos, R.; Meetsma, A.; Teuben, J. H. *Organometallics* **1991**, *10*, 2665. (d) Adams, R. D.; Chodosh, D. F. *Inorg. Chem.* **1978**, *17*, 41.

(17) Usón, R.; Fornies, J.; Espinet, P.; Lalinde, E.; Jones, P.; Sheldrick, G. M. *J. Organomet. Chem.* **1985**, *288*, 249.

(18) (a) Carmona, E.; Palma, P.; Poveda, M. L. *Polyhedron* **1990**, *9*, 1447. (b) Maddock, S. M.; Rickard, C. E. F.; Roper, W. R.; Wright, L. J. *J. Organomet. Chem.* **1996**, *510*, 267. (c) Mantovani, A.; Calligaro, L.; Pasquetto, A. *Inorg. Chim. Acta* **1983**, *76*, L145.

Table 7. Crystal and Refinement Data for **2**

	2c	3c	3h
formula	C ₁₃ H ₂₄ Br ₂ P ₂ Pd	C ₁₈ H ₃₃ Br ₂ NP ₂ Pd	C ₂₄ H ₄₅ Br ₂ NP ₂ Pd
mol wt	508.48	591.621	675.77
crystal system	monoclinic	orthorhombic	monoclinic
space group	<i>P</i> 2 ₁ / <i>c</i>	<i>Pbcn</i>	<i>P</i> 2 ₁ 2 ₁ 2 ₁
cell dimensions			
<i>a</i> , Å	11.3000(10)	30.611(3)	19.887(2)
<i>b</i> , Å	12.3990(10)	12.453(1)	16.928(2)
<i>c</i> , Å	14.257(2)	12.946(1)	9.130(2)
α, deg	90	90	90
β, deg	109.260(10)	90	90
γ, deg	90	90	90
<i>Z</i>	4	8	4
<i>V</i> , Å ³	1885.7(3)	4935.00(73)	3073.6(8)
<i>D</i> _{calc} , g cm ⁻³	1.791	1.5926	1.460
abs coeff, mm ⁻¹	5.376	4.1219	3.319
<i>F</i> (000)	992	2352.0	1368
temp, K	293(2)	293(2)	293(2)
wavelength, Å	0.71070	0.71070	0.71070
crystal size, mm	0.21 × 0.20 × 0.18	0.20 × 0.30 × 0.18	0.17 × 0.22 × 0.19
θ range for data collection, deg	2.23–27.00	2–26	2.05–24.97
index ranges	0 ≤ <i>h</i> ≤ 14, 0 ≤ <i>k</i> ≤ 15, –8 ≤ <i>l</i> ≤ 8	0 ≤ <i>h</i> ≤ 38, 0 ≤ <i>k</i> ≤ 16, –8 ≤ <i>l</i> ≤ 15	0 ≤ <i>h</i> ≤ 23, 0 ≤ <i>k</i> ≤ 20, –8 ≤ <i>l</i> ≤ 10
no. of reflns collected	2436	5370	3045
no. of indep reflns	2436	2583	3045
	[<i>R</i> (int) = 0.0000]		[<i>R</i> (int) = 0.0000]
refinement method	full-matrix least-squares on <i>F</i> ²	full-matrix least-squares on <i>F</i> ²	full-matrix least-squares on <i>F</i> ²
no. of data/restraints/params	2436/0/163	2583/0/217	3045/0/271
goodness-of-fit on <i>F</i> ²	2.076		1.133
final <i>R</i> indices [<i>I</i> > 2σ(<i>I</i>)]	<i>R</i> 1 = 0.0775, <i>wR</i> 2 = 0.2156	<i>R</i> 1 = 0.074, <i>R</i> _w = 0.083	<i>R</i> 1 = 0.0662, <i>wR</i> 2 = 0.1943
<i>R</i> indices (all data)	<i>R</i> 1 = 0.0990, <i>wR</i> 2 = 0.2770		<i>R</i> 1 = 0.0892, <i>wR</i> 2 = 0.2258
largest diff peak and hole, e Å ⁻³	0.723 and –1.662	0.702 and –0.501	0.771 and –0.703
max absorp corr		1.350	
min absorp corr		0.665	
av absorp corr		0.963	

Table 8. Selected Bond Distances and Angles for **2c**

bond distances (Å)		bond angles (deg)	
Pd(1)–C(1)	2.078(13)	C(1)–Pd(1)–P(1)	88.7(5)
Pd(1)–P(1)	2.307(5)	C(1)–Pd(1)–P(2)	90.7(6)
Pd(1)–P(2)	2.297(6)	P(1)–Pd(1)–P(2)	177.91(13)
Pd(1)–Br(1)	2.520(2)	C(1)–Pd(1)–Br(1)	178.2(4)
C(1)–C(2)	1.48(2)	P(1)–Pd(1)–Br(1)	91.87(11)
		P(2)–Pd(1)–Br(1)	88.70(14)
		C(2)–C(1)–Pd(1)	117.4(9)

Table 9. Selected Bond Distances and Angles for **3c**

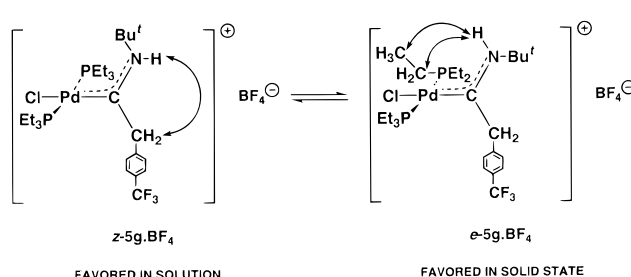
bond distances (Å)		bond angles (deg)	
Pd(1)–C(1)	2.012(4)	C(1)–Pd(1)–P(1)	90.5(4)
Pd(1)–P(1)	2.317(4)	C(1)–Pd(1)–P(2)	88.6(4)
Pd(1)–P(2)	2.326(4)	P(1)–Pd(1)–P(2)	178.1(2)
Pd(1)–Br(1)	2.572(2)	C(1)–Pd(1)–Br(1)	176.5(4)
C(1)–C(2)	1.58(2)	P(1)–Pd(1)–Br(1)	89.4(1)
N(1)–C(1)	1.24(2)	P(2)–Pd(1)–Br(1)	91.4(1)
N(1)–C(9)	1.49(2)	C(2)–C(1)–Pd(1)	108.3(8)
C(2)–C(3)	1.50(2)	N(1)–C(1)–Pd(1)	135.8(1)
		N(1)–C(1)–C(2)	115.7(1)
		C(1)–N(1)–C(9)	127.7(1)

Thus, when a solid crystalline sample of this compound is dissolved in CD₂Cl₂ at room temperature and the ¹H NMR is immediately recorded, two sets of signals are seen, which correspond to two isomers in a ca. 10:1 ratio. Within 24 h, the signals corresponding to the minor isomer grow at the expense of the major, inverting the proportion, until a final equilibrium ratio of ca. 0.05:1 is reached. The initial situation is restored if the sample is crystallized and dissolved again in CD₂Cl₂. As represented in Scheme 6, 2D-NOESY experiments carried

Table 10. Selected Bond Distances and Angles for **3h**

bond distances (Å)		bond angles (deg)	
Pd(1)–C(1)	2.05(2)	C(1)–Pd(1)–P(1)	91.3(5)
Pd(1)–P(1)	2.332(5)	C(1)–Pd(1)–P(2)	89.8(5)
Pd(1)–P(2)	2.329(5)	P(1)–Pd(1)–P(2)	178.8(2)
Pd(1)–Br(1)	2.513(2)	C(1)–Pd(1)–Br(1)	171.9(5)
C(1)–C(2)	1.35(2)	P(1)–Pd(1)–Br(1)	90.16(14)
N(1)–C(1)	1.39(2)	P(2)–Pd(1)–Br(1)	88.73(13)
N(1)–C(9)	1.52(2)	C(2)–C(1)–Pd(1)	126.9(14)
C(2)–C(3)	1.44(2)	N(1)–C(1)–Pd(1)	107.6(11)
		N(1)–C(1)–C(2)	126(2)
		C(1)–N(1)–C(9)	127.0(14)

Scheme 6



out with solutions of **5g**·BF₄ allow the identification of the two rotamers. It is found that whereas that favored in solution exhibits a *z* configuration of the *t*-Bu and [Pd] fragments across the C–N bond, the one preferred in the solid state has an *e* distribution of these groups.

The use of a weaker acid such as HOAc leads to partial protonation and to the formation of equilibrium mixtures of the corresponding imine, enamine, and amidocarbene species (Scheme 7). Figure 4 shows the

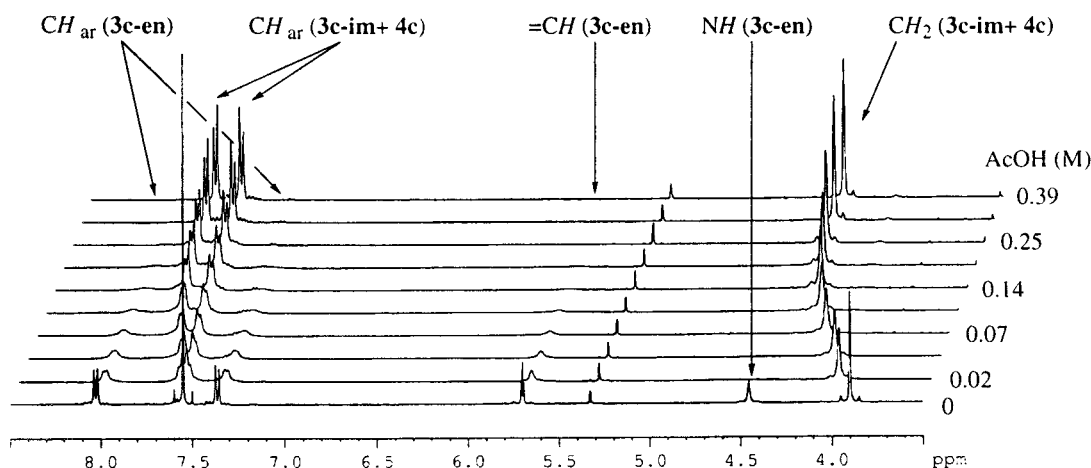
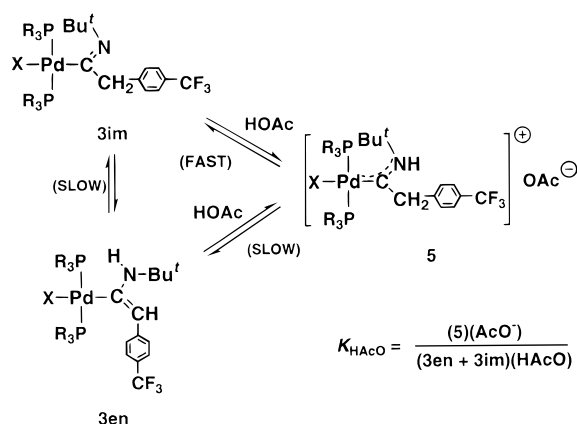


Figure 4. ^1H spectrum of **3o** (0.083 M in CD_2Cl_2) in the presence of increasing concentrations of acetic acid (0–0.39 M).

Scheme 7

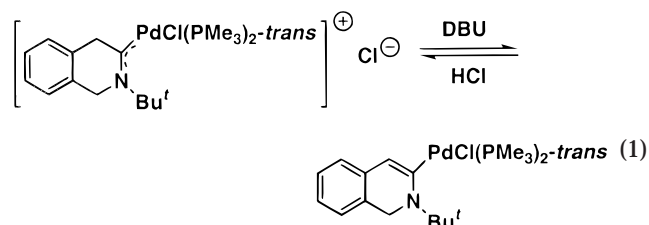


effect of successive additions of acetic acid to a solution of compound **3o** in CD_2Cl_2 . The amino carbene complex **5** and the corresponding imidoyl **3im** undergo a very fast exchange and consequently furnish an averaged set of signals, but the proton exchanges that involve the enamine tautomer are slow on the NMR time scale. This is not unexpected¹⁹ since proton exchange at nitrogen is usually much faster than at carbon centers, due to the higher electronegativity of the former and to the presence of a lone pair.¹⁹ Accordingly, the CH_2 signal of the methylene group of **3o-im**, which appears at 3.96 ppm in neat CD_2Cl_2 , is displaced to lower field upon addition of acetic acid, until it reaches a constant chemical shift of 4.38 ppm, which corresponds to the methylene group of the amidocarbene complex **5o-AcO**. Due to its slow rate of proton exchange, the signals of the enamine **3o-en** remain only slightly broadened and do not shift on addition of AcOH, allowing the determination of the concentration of the species involved in these equilibria.

Similar experiments have been carried out with complexes **3b**, **3g**, **3i**, and **3j**, although reliable equilibrium constants could not be calculated, probably due to ion-pairing effects in the solvent used (CD_2Cl_2).²⁰ However, from the extrapolation to zero concentration of AcOH, the equilibrium constant K_{AcOH} can be estimated to be in the range 0.1–0.01 for these complexes,

and therefore, the imidoyl complexes are somewhat weaker bases than the acetate anion.

Imine/Enamine Tautomerism of Imidoyl Complexes. When imidoyl complexes of type **3** are dissolved in slightly wet acetone- d_6 , an equilibrium mixture of the imine and enamine tautomers is rapidly attained. Allowing these solutions to stand for extended periods of time (1–2 days) does not result in any significant change of the imine/enamine ratio. The values of the equilibrium constants ($K_{\text{im/en}}$ = (imine)/(enamine)) in acetone- d_6 for complexes **3a–o** are listed in Table 3. The addition of anhydrous CD_2Cl_2 to a pure, crystalline sample of **3b-en** gives a solution that contains the enamine tautomer exclusively. However, the presence of small amounts of water (1 μL) catalyzes the conversion of **3b-en** into **3b-im**, and an equilibrium enamine:imine ratio of 0.9:1 is reached within 2 h. Accordingly, as in the case of the related keto/enol or imine/enamine tautomerism of organic compounds,^{4,21} a general acid (path A) or base (path B) catalyzed mechanism could be proposed for the proton exchange in compounds of type **3** (Scheme 8). Although the deprotonation of transition metal acyl derivatives is a well-known process,²² we favor path A over path B because the former appears to be more in accordance with the chemical properties of palladium imidoyl complexes. For instance, as already discussed, Pd-imidoyls are readily protonated even by weak acids such as HOAc. In addition, we have recently shown that the methylene group of an *N,N*-dialkylaminocarbene palladium complex can be deprotonated with DBU to yield the corresponding enamine (eq 1).⁹



Studies on the imine/enamine tautomerism of organic imines have shown that the electronic properties of the substituents of the imine/enamine functionality have a

(19) Kramarz, K. W.; Norton, J. R. *Prog. Inorg. Chem.* **1994**, *42*, 1.

(20) Ritchie, C. D. In *Physical Organic Chemistry*; Marcel Dekker: New York, 1990.

(21) Lowry, T. H.; Schueller Richardson, K. In *Mechanism and Theory in Organic Chemistry*; Harper and Row: New York, 1987.

Scheme 8

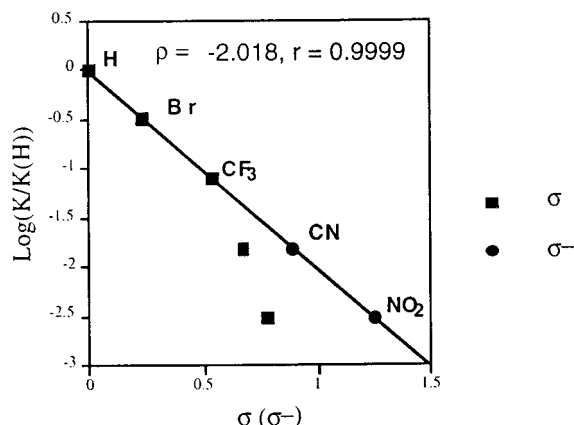
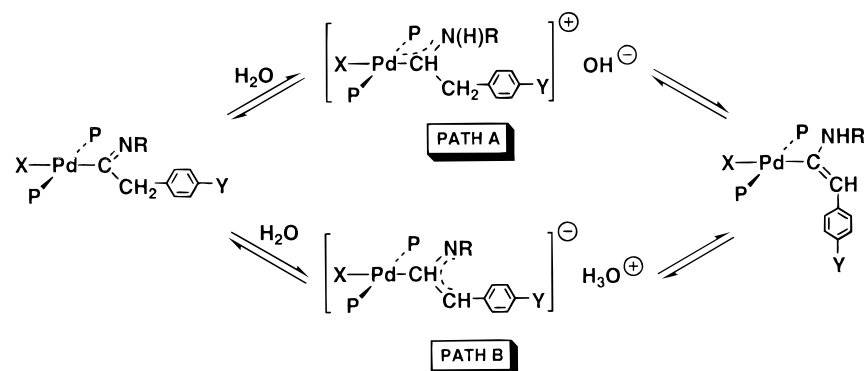
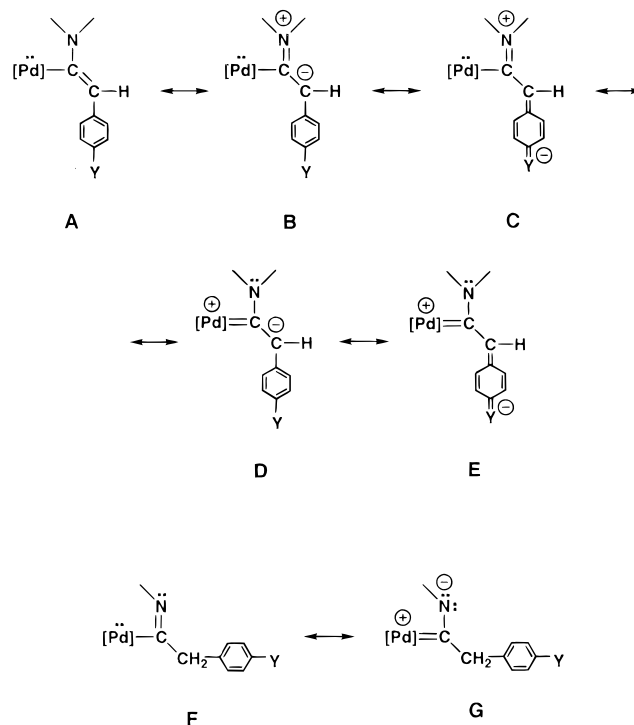


Figure 5. Hammett plot for the imine/enamine ratio in acetone- d_6 .

considerable influence on the equilibrium position.⁵ To ascertain whether a comparable effect could also be found in organometallic derivatives, we have prepared a series of five, closely related iminoacyl complexes (**3c**, **3e**, **3f**, **3n**, **3o**) that contain the same halogen (Br) and phosphine ligands (PMe_3) and differ only in the nature of the para-substituent on the aromatic ring (Br, NO_2 , CN, H, and CF_3 , respectively). Electron-withdrawing groups favor the formation of the enamine form in such a manner that, while for compound **3o** a very small amount on the enamine tautomer can be detected in solution in acetone- d_6 (ca. 9%), for the nitro derivative the opposite situation holds (ca. 97%). The representation of the logarithm of the imine/enamine equilibrium constant in the same solvent versus the Hammett σ parameter²³ (Figure 5) shows an excellent correlation for the substituents p -H, p -Br, and p - CF_3 . The groups p -CN and p - NO_2 deviate considerably, but if the σ^- parameter, which takes into account the possible electronic conjugation with the lone pair of the enamine nitrogen atom (resonance form C, Chart 2), is used instead, a very good correlation is found. The effect of electron-withdrawing substituents on the aromatic ring of the ligand can be rationalized in terms of the stabilization of the negative charge on the methyne group, as represented by the resonance structures B and D (Chart 2).

Chart 2



The influence of the [Pd] fragment on the value of $K_{im/en}$ is less clear than that of the aromatic ring substituents and requires some additional considerations. It might be argued that an electron-rich metal center could stabilize the electronically highly delocalized enamine tautomer to a larger extent than the imine form (see Chart 2), but this hypothesis fails to provide an explanation for the im/en ratio of ca. 0.3 found for compounds **3i**, **3j**, and **3k**, which contain aryl phosphines of the type PMe_2Ar . In addition, whereas no correlation can be found between $K_{im/en}$ and the donor/acceptor ability of the phosphine (represented by the value of $\nu(CO)$ in $Ni(CO)_3(PR_3)$,²⁴ see Table 6), a better defined relationship may exist between $K_{im/en}$ and the phosphine cone angle^{24a,25} since the smaller values of the equilibrium constant appear associated with the more sterically demanding phosphines. It is possible that the steric pressure introduced by the bulky phos-

(22) (a) Liebeskind, L. S.; Welker, M. E.; Fengl, R. W. *J. Am. Chem. Soc.* **1986**, *108*, 6328. (b) Rusik, C. A.; Collins, M. A.; Gamble, A. S.; Tonker, T. L.; Templeton, T. L. *J. Am. Chem. Soc.* **1989**, *111*, 2250. (c) Fermin, M.; Thiyagarajan, B.; Bruno, J. W. *J. Am. Chem. Soc.* **1993**, *115*, 974.

(23) Hansch, C.; Leo, A.; Taft, W. R. *Chem. Rev.* **1991**, *91*, 165.

(24) (a) Tolman, C. A. *Chem. Rev.* **1977**, *77*, 313. (b) Jolly, P. W. In *Comprehensive Organometallic Chemistry*; Wilkinson, G., Stone, F. G. A., Abel, E. W., Eds.; Pergamon Press: New York, 1982; Vol. 6.

(25) White, D.; Coville, N. J. *Adv. Organomet. Chem.* **1994**, *36*, 95.

phines in the already congested iminoacyl tautomers (recall that the bulky *t*-Bu group of the iminoacyl has a *z* distribution with regard to the [Pd] moiety) favors tautomerization to the less hindered enamine tautomer. In accord with these considerations the substitution of the *t*-Bu group of **3b** ($\text{PR}_3 = \text{PMe}_3$; $\text{X} = \text{Cl}$; $\text{Y} = \text{CF}_3$) by a less bulky *i*-Pr substituent at the isocyanide nitrogen compound (**3m**) leads to a increase of about 1 order of magnitude in the value of $K_{\text{im/en}}$ (from 0.7 in **3b** to 6.7 in **3m**, see Table 3).

Conclusions

Palladium imidoyl complexes can exist in tautomeric imine and enamine forms. As in the related tautomeric equilibria of organic imines, the exchange is catalyzed by small amounts of protic acids present in solution, including water. While the imine tautomer is in general more stable, under certain circumstances the enamine form is preferred. Thus, the presence of electron acceptor substituents on the imidoyl functionality favor the enamine form. Since the influence of the metal fragment on the equilibrium seems to be small and mostly of steric origin, this kind of tautomerism resembles the more general imine/enamine tautomerism of organic imines. It is reasonable to expect that similar tautomeric equilibria can be found in other organometallic complexes containing imidoyl or related ligands and that such equilibria may influence the chemical reactivity of these complexes.

Experimental Section

Microanalyses were performed by the Analytical Service of the University of Sevilla and the Instituto de Investigaciones Químicas. The spectroscopic instruments used were Perkin-Elmer models 684 and 883 and Bruker model Vector 22 for IR spectra and Bruker AMX-300, DRX-400, AMX-500, and DRX-500 for NMR spectroscopy. The ^{13}C resonance of the solvent was used as an internal standard, but chemical shifts are reported with respect to SiMe_4 . The $^{13}\text{C}\{^1\text{H}\}$ NMR assignments were helped in most cases with the use of gate decoupling techniques. $^{31}\text{P}\{^1\text{H}\}$ NMR shifts are referenced to external 85% H_3PO_4 . All preparations and other operations were carried out under oxygen-free nitrogen by conventional Schlenk techniques. Solvents were dried and degassed before use. The petroleum ether used had a boiling point of 40–60 °C. Phosphines $\text{Me}_2\text{PC}_6\text{H}_4\text{-}p\text{-NMe}_2$ and $\text{Me}_2\text{PC}_6\text{H}_4\text{-}p\text{-F}$ were prepared by reacting Me_2PCl with the Grignard reagents $\text{ClMgC}_6\text{H}_4\text{-}p\text{-NMe}_2$ and $\text{ClMgC}_6\text{H}_4\text{-}p\text{-F}$, respectively. Compounds $\text{Pd}(\eta^2\text{-CH}_2=\text{CH-CO}_2\text{Me})(\text{PR}_3)_2$ ($\text{R} = \text{Et}$, Me_2Ph , $\text{Me}_2\text{PC}_6\text{H}_4\text{-}p\text{-NMe}_2$, $\text{Me}_2\text{PC}_6\text{H}_4\text{-}p\text{-F}$) were prepared according to the reported procedure for $\text{Pd}(\eta^2\text{-CH}_2=\text{CH-CO}_2\text{Me})(\text{PMe}_3)_2$.⁹

The preparation of compounds **2a–I** involves the reaction of $\text{Pd}(\eta^2\text{-CH}_2=\text{CH-CO}_2\text{Me})(\text{PR}_3)_2$ ($\text{R} = \text{Me}$, Et , Me_2Ph , $\text{Me}_2\text{PC}_6\text{H}_4\text{-}p\text{-NMe}_2$, $\text{Me}_2\text{PC}_6\text{H}_4\text{-}p\text{-F}$) with the appropriate benzyl halide. The subsequent treatment of these complexes with the isonitrile ($\text{Bu}'\text{NC}$ or $\text{Pr}'\text{NC}$) affords the corresponding iminoacyl derivatives. A representative example of the experimental procedure employed to synthesize **2a** and **3a(im/en)** is as follows.

2a. To a cold (−30 °C) solution of $\text{Pd}(\eta^2\text{-CH}_2=\text{CH-CO}_2\text{Me})(\text{PMe}_3)_2$ (0.17 g, 0.5 mmol) in THF (30 mL) was added $\text{ClCH}_2\text{C}_6\text{H}_4\text{-}p\text{-CF}_3$ (75 μL , 0.5 mmol). The cooling bath was removed and the mixture stirred at room temperature for 4 h. The solution was then taken to dryness and the residue extracted with diethyl ether. After filtration, the solvent was evaporated and the compound obtained as pale yellow crystals in 70% yield.

3a. $\text{Bu}'\text{NC}$ (0.34 mmol, 0.34 mL of a 1 M solution in toluene) was added to a solution of **2a** (0.15 g, 0.34 mmol) in Et_2O (30 mL). The solution was stirred at room temperature for 3 h, the solvent removed under vacuum, and the residue extracted with Et_2O . Filtration, concentration of the filtrate, and addition of some petroleum ether provided yellow crystals of the complex after cooling at −30 °C for several hours. Yield: 71%.

The bromide derivatives **3n** and **3o** were prepared from the analogous chlorides, **3a** and **3b**, by stirring with KBr in acetone, at room temperature, for 12 h.

Tables 1–5 collect analytical and spectroscopic (IR and NMR) data, for the new compounds described.

4. A solution of $\text{Pd}(\eta^2\text{-CH}_2=\text{CH-CO}_2\text{Me})(\text{PMe}_3)_2$ (0.5 g, 1.45 mmol) in THF (30 mL) was treated with $\text{ClCH}_2\text{C}_6\text{H}_4\text{-}p\text{-CF}_3$ (0.21 mL, 1.45 mmol) and dmpe (1.45 mmol, 2.9 mL of a 0.5 M solution in toluene). The resulting mixture was stirred at room temperature for 30 min and then taken to dryness. Extraction with a mixture of toluene– CH_2Cl_2 (1:1), centrifugation, and concentration provided pale yellow crystals of **4** after cooling at −30 °C. Yield: 60%. Anal. Calcd for $\text{C}_{22}\text{H}_{40}\text{ClF}_3\text{NP}_3$: Pd: C, 43.3; H, 6.6; N, 2.3. Found: C, 43.6; H, 6.4; N, 2.6. IR (Nujol mull, cm^{-1} , $\nu(\text{NH})$) 3280 (b). ^1H NMR (CDCl_3 , 20 °C): δ 1.06 (dd, 3 H, $^2J_{\text{HP}} = 10.2$, $^4J_{\text{HP}} = 2.5$ Hz, P–Me), 1.41 (s, 9 H, CMe_3), 1.45 (dd, 3 H, $^2J_{\text{HP}} = 9.7$, $^4J_{\text{HP}} = 2.4$ Hz, PMe_3), 1.48 (d, 3 H, $^2J_{\text{HP}} = 8.5$ Hz, P–Me), 1.65 (m, 2 H, P– CH_2), 1.80 (dd, 3 H, $^2J_{\text{HP}} = 11.5$, $^4J_{\text{HP}} = 2.3$ Hz, P–Me), 1.86 (d, 3 H, $^2J_{\text{HP}} = 9.6$ Hz, P–Me), 2.20 (m, 2 H, P– CH_2), 5.93 (dt, 1 H, $^4J_{\text{HP}} = 19.4$, $^4J_{\text{HP}} = 2.8$ Hz, CH), 6.60 (d, 1 H, $^4J_{\text{HP}} = 5.6$ Hz, NH), 7.14 (d, 2 H, $^3J_{\text{HH}} = 8.6$ Hz, CH_{ar}), 7.57 (d, 2 H, $^3J_{\text{HH}} = 7.4$ Hz, CH_{ar}). $^{31}\text{P}\{^1\text{H}\}$ NMR (CDCl_3 , 20 °C): AMX spin system, $\delta_{\text{A}} = -22.1$, $\delta_{\text{M}} = 22.1$, $\delta_{\text{X}} = 30.2$, $J_{\text{AX}} = 364$, $J_{\text{AM}} = 37$, $J_{\text{MX}} = 27$ Hz. $^{13}\text{C}\{^1\text{H}\}$ NMR (CDCl_3 , 20 °C): δ 11.8 (d, $^1J_{\text{CP}} = 27$ Hz, P–Me), 12.8 (d, $^1J_{\text{CP}} = 29$ Hz, P–Me), 14.2 (d, $^1J_{\text{CP}} = 20$ Hz, P–Me), 15.0 (d, $^1J_{\text{CP}} = 21$ Hz, P–Me), 16.0 (d, $^1J_{\text{CP}} = 27$ Hz, PMe_3), 27.9 (dd, $^1J_{\text{CP}} = 31$, $^2J_{\text{CP}} = 20$ Hz, P– CH_2), 28.9 (ddd, $^1J_{\text{CP}} = 25$, $^2J_{\text{CP}} = 16$, $^3J_{\text{CP}} = 5$ Hz, P– CH_2), 29.3 (s, CMe_3), 53.2 (d, $^4J_{\text{CP}} = 7$ Hz, CMe_3), 100.6 (s, CH), 120.3 (q, $^2J_{\text{CF}} = 31$ Hz, C– CF_3), 121.8 (bs, 2 C_{arH}), 124.4 (d, $^4J_{\text{CF}} = 3$ Hz, 2 C_{arH}), 148.7 (s, C_{ar}), 169.1 (d, $^2J_{\text{CP}} = 108$, CN).

5g·BF₄. HBF_4 (0.6 mmol, 0.12 mL of a 35% solution in water) was added to a solution of **3g** (0.37 g, 0.6 mmol) in Et_2O (30 mL). A white solid precipitated following the addition of the acid. The suspension was stirred at room temperature for 2 h. The solvent was filtered and the solid recrystallized from $\text{CH}_2\text{Cl}_2\text{-Et}_2\text{O}$ (1:1) and obtained as white crystals in 80% yield.

Complex **5b·BF₄** was similarly prepared starting from **3b** and HBF_4 and isolated as pale yellow crystals in 85% yield.

5b·BF₄. Anal. Calcd for $\text{C}_{19}\text{H}_{34}\text{BClF}_7\text{NP}_2\text{Pd}$: C, 36.5; H, 5.4; N, 2.2. Found: C, 36.3; H, 5.4; N, 2.2. IR (Nujol mull, cm^{-1} , $\nu(\text{NH})$) 3222 (b). ^1H NMR (CD_2Cl_2 , 20 °C): δ 1.30 (t, 6 H, $^*J_{\text{HP}} = 3.7$ Hz, PMe_3), 1.69 (s, 9 H, CMe_3), 4.19 (bs, 2 H, CH_2), 10.62 (bs, 1 H, NH), 7.71 (d, 2 H, $^3J_{\text{HH}} = 8.2$ Hz, CH_{ar}), 7.78 (d, 2 H, $^3J_{\text{HH}} = 8.2$ Hz, CH_{ar}). $^{31}\text{P}\{^1\text{H}\}$ NMR (CD_2Cl_2 , 20 °C): δ −15.1 (s, PMe_3). $^{13}\text{C}\{^1\text{H}\}$ NMR (CD_2Cl_2 , 20 °C): δ 13.9 (t, $^*J_{\text{CP}} = 16$ Hz, PMe_3), 29.1 (s, CMe_3), 55.1 (s, CH_2), 60.7 (s, CMe_3), 126.3 (s, 2 C_{arH}), 131.4 (s, 2 C_{arH}), 139.2 (s, C_{ar}), 231.0 (s, CN).

5g·BF₄. Anal. Calcd for $\text{C}_{25}\text{H}_{46}\text{BClF}_7\text{NP}_2\text{Pd}$: C, 42.4; H, 6.5; N, 2.0. Found: C, 42.1; H, 6.1; N, 2.0. IR (Nujol mull, cm^{-1} , $\nu(\text{NH})$) 3303 (b).

z-5g·BF₄. ^1H NMR (CD_2Cl_2 , 20 °C): δ 1.16 (pq, 18 H, $^*J_{\text{HP}} \approx ^3J_{\text{HH}} = 8.0$ Hz, Me (PET_3)), 1.68 (m, 6 H, CH_2 (PET_3)), 1.72 (s, 9 H, CMe_3), 1.79 (m, 6 H, CH_2 (PET_3)), 4.38 (s, 2 H, CH_2), 10.28 (bs, 1 H, NH), 7.58 (d, 2 H, $^3J_{\text{HH}} = 8.0$ Hz, CH_{ar}), 7.73 (d, 2 H, $^3J_{\text{HH}} = 8.1$ Hz, CH_{ar}). $^{31}\text{P}\{^1\text{H}\}$ NMR (CD_2Cl_2 , 20 °C): δ 11.7 (s, PET_3). $^{13}\text{C}\{^1\text{H}\}$ NMR (CD_2Cl_2 , 20 °C): δ 8.9 (s, Me (PET_3)), 16.2 (t, $^*J_{\text{CP}} = 14$ Hz, CH_2 (PET_3)), 28.9 (s, CMe_3), 55.5 (s, CH_2), 61.0 (s, CMe_3), 124.2 (q, $^1J_{\text{CF}} = 272$ Hz, CF_3), 126.8 (q, $^4J_{\text{CF}} = 5$ Hz, 2 C_{arH}), 131.2 (s, 2 C_{arH}), 137.0 (s, C_{ar}), 228.4 (pt, $^2J_{\text{CP}} = 5$ Hz, CN).

e-5g·BF₄. ^1H NMR (CD_2Cl_2 , 20 °C): δ 1.07 (pq, 18 H, $^*J_{\text{HP}} \approx ^3J_{\text{HH}} = 8.0$ Hz, Me (PET_3)), 1.58 (m, 6 H, CH_2 (PET_3)), 1.74

(s, 9 H, CMe₃), 1.76 (m, 6 H, CH₂ (PEt₃)), 4.13 (s, 2 H, CH₂), 10.06 (bs, 1 H, NH), 7.72 (d, 2 H, ³J_{HH} = 8.3 Hz, CH_{ar}), 7.79 (d, 2 H, ³J_{HH} = 8.1 Hz, CH_{ar}). ³¹P{¹H} NMR (CD₂Cl₂, 20 °C): δ 10.0 (s, PEt₃). ¹³C{¹H} NMR (CD₂Cl₂, 20 °C): δ 8.3 (s, Me (PEt₃)), 15.2 (t, *J_{CP} = 14 Hz, CH₂ (PEt₃)), 30.3 (s, CMe₃), 49.5 (s, CH₂), 64.8 (s, CMe₃), 126.8 (s, 2 C_{ar}H), 130.9 (s, 2 C_{ar}H), 139.3 (s, C_{ar}), 240.7 (s, CN).

X-ray Structure Determination of Compounds 2c, 3c, and 3h. A summary of the fundamental crystal data is given in Table 7. Data were collected from single crystals of dimensions (0.22 × 0.19 × 0.20 mm, **2c**; 0.20 × 0.30 × 0.18 mm, **3c**; 0.20 × 0.30 × 0.18 mm, **3h**) on a PW-1100 diffractometer, using graphite-monochromated Mo Kα radiation. A total of 2546 (**2c**), 5370 (**3c**), and 3070 (**3h**) independent reflections were measured, 2436 (**2c**), 2583 (**3c**), and 3045 (**3h**) of which were considered as observed using the criterion $I \geq 2\sigma(I)$. Scattering factors, dispersion corrections, and absorption coefficients were taken from International Tables for Crystallography.²⁶ The structure was solved by Patterson methods and Fourier synthesis, and most of the calculations were performed by using XRAY80²⁷ and DIRDIF.²⁸ The structure was refined by least-squares analysis using unit weights with anisotropic parameters for non-H atoms. The positions of the

hydrogen atoms were refined with distance restraints for the C–H distances. No extinction corrections were applied. The absorption correction was carried out by using DIFABS.²⁹

Acknowledgment. Financial support from the Dirección General de Investigación Científica y Técnica (Proyecto PB96-0824) and Junta de Andalucía is gratefully acknowledged. S.A.H. thanks the Commission of the European Union for a grant from the HCM program (Project No. ERCHBICT920061). C.M.D. thanks the Dirección General de Enseñanza Superior for a PFPI studentship. Thanks are also due to the University of Sevilla and the Instituto de Investigaciones Químicas for free access to the analytical and NMR facilities.

Supporting Information Available: Tables of atomic coordinates, thermal parameters, and bond lengths and angles for **2c**, **3c**, and **3h**. This material is available free of charge via the Internet at <http://pubs.acs.org>.

OM9905557

(26) *(26)International Tables for Crystallography*; C. Kluwer Academic Publishers: Dordrecht, 1992.

(27) Stewart, J. M.; Machin, P. A.; Dickinson, C. W.; Ammon, H. L.; Heck, H.; Flack, H. In *The X-ray System. Technical Report TR-446*; Computer Science Centre: University of Maryland, 1976.

(28) Beurskens, P. T.; Bosman, W. P.; Doesburg, H. M.; Gould, R. O.; Van den Hark, Th. E. M.; Prick, P. A. J.; Noordik, J. H.; Beurskens, G.; Parthasarathi, V.; Bruins Slot, H. J.; Hiltiwanger, R. C.; Smits, J. M. M. In *DirDif System*; Crystallography Laboratory, Toernooiveld, Nijmegen, The Netherlands, 1984.

(29) Walker, N.; Stuart, D. *DIFABS. Acta Crystallogr.* **1983**, *A39*, 158.